ANNALS of Clinical and Translational Neurology
Open Access
ANA American Neurological Association since 1875

RESEARCH ARTICLE

Endplate denervation correlates with Nogo-A muscle expression in amyotrophic lateral sclerosis patients

Gaëlle Bruneteau[1,2,3], Stéphanie Bauché[1], Jose Luis Gonzalez de Aguilar[4,5], Guy Brochier[6,7], Nathalie Mandjee[1], Marie-Laure Tanguy[8], Ghulam Hussain[4,5], Anthony Behin[7], Frédéric Khiami[9], Elhadi Sariali[9], Caroline Hell-Remy[10], François Salachas[2], Pierre-François Pradat[2], Lucette Lacomblez[2], Sophie Nicole[1], Bertrand Fontaine[1], Michel Fardeau[6], Jean-Philippe Loeffler[4,5], Vincent Meininger[2], Emmanuel Fournier[1,7], Jeanine Koenig[1] & Daniel Hantaï[1,7]

[1]Inserm U 1127, CNRS UMR 7225, Sorbonne Universités, UPMC Univ Paris 06, UMR S 1127, Institut du Cerveau et de la Moelle épinière, ICM, F-75013, Paris, France
[2]APHP, Hôpital Pitié-Salpêtrière, Département des Maladies du Système Nerveux, Centre référent SLA, Paris, France
[3]APHP, INSERM, ICM, Centre d'Investigation Clinique Pitié Neurosciences, CIC-1422, Département des Maladies du Système Nerveux, Hôpital Pitié-Salpêtrière, Paris, France
[4]Université de Strasbourg, UMR_S 1118, Strasbourg, France
[5]INSERM, U1118, Mécanismes Centraux et Périphériques de la Neurodégénérescence, Strasbourg, France
[6]Unité de Morphologie Neuromusculaire, Institut de Myologie, Hôpital Pitié-Salpêtrière, Paris, France
[7]APHP, Hôpital Pitié-Salpêtrière, Centre de référence de pathologie neuromusculaire Paris-Est, Institut de Myologie, Paris, France
[8]AP-HP, Hôpital Pitié-Salpêtrière, Unité de Recherche Clinique, Paris, France
[9]APHP, Hôpital Pitié-Salpêtrière, Service d'Orthopédie, Paris, France
[10]APHP, Hôpital Pitié-Salpêtrière, Département d'Anesthésie-Réanimation, Paris, France

Correspondence
Gaëlle Bruneteau, Département des Maladies du Système nerveux, Centre Référent SLA, Hôpital Pitié-Salpêtrière, 47-83 Bd de l'Hôpital, 75013 Paris, France. Tel: +33 142 162471; Fax: +33 142 162473; E-mail: gaelle.bruneteau@psl.aphp.fr

Funding Information
This work was supported by the Association Française pour la Recherche sur la SLA (ARSla, AO 2007 – NETALS; G. B., D. H.), the Association Française contre les Myopathies (AFM, AO 2008 – no. 13501; G. B.), the Agence Nationale de la Recherche (ANR, program "Investissements d'avenir" ANR-10-IAIHU-06; D. H., B. F.), the European Community's Health Seventh Framework Programme under Grant agreement no. 259867 (J.-P. L.), and a "Contrat d'interface" Inserm/APHP to G. B. Jose Luis Gonzalez de Aguilar is the recipient of a "Chaire d'Excellence INSERM/Université de Strasbourg."

Received: 31 December 2014; Accepted: 1 January 2015

Annals of Clinical and Translational Neurology **2015; 2(4): 362–372**

doi: 10.1002/acn3.179

Abstract

Objective: Data from mouse models of amyotrophic lateral sclerosis (ALS) suggest early morphological changes in neuromuscular junctions (NMJs), with loss of nerve–muscle contact. Overexpression of the neurite outgrowth inhibitor Nogo-A in muscle may play a role in this loss of endplate innervation. **Methods**: We used confocal and electron microscopy to study the structure of the NMJs in muscle samples collected from nine ALS patients (five early-stage patients and four long-term survivors). We correlated the morphological results with clinical and electrophysiological data, and with Nogo-A muscle expression level. **Results**: Surface electromyography assessment of neuromuscular transmission was abnormal in 3/9 ALS patients. The postsynaptic apparatus was morphologically altered for almost all NMJs (n = 430) analyzed using confocal microscopy. 19.7% of the NMJs were completely denervated (fragmented synaptic gutters and absence of nerve terminal profile). The terminal axonal arborization was usually sparsely branched and 56.8% of innervated NMJs showed a typical reinnervation pattern. Terminal Schwann cell (TSC) morphology was altered with extensive cytoplasmic processes. A marked intrusion of TSCs in the synaptic cleft was seen in some cases, strikingly reducing the synaptic surface available for neuromuscular transmission. Finally, high-level expression of Nogo-A in muscle was significantly associated with higher extent of NMJ denervation and negative functional outcome. **Interpretation**: Our results support the hypothesis that morphological alterations of NMJs are present from early-stage disease and may significantly contribute to functional motor impairment in ALS patients. Muscle expression of Nogo-A is associated with NMJ denervation and thus constitutes a therapeutic target to slow disease progression.

Introduction

Amyotrophic lateral sclerosis (ALS) is a progressive neurodegenerative disorder involving motor neurons of the cerebral cortex, brain stem, and spinal cord, usually leading to death in 3–5 years.[1,2] The cause of the disease is unknown and about 90% of ALS cases are sporadic. The remaining 10% are familial cases among which 20% can be attributed to a mutation in the superoxide dismutase (*SOD1*) gene. Several lines of evidence suggest early and selective changes in neuromuscular junctions (NMJs) in ALS. Studies using transgenic mice expressing mutations in the *SOD1* gene have shown that NMJ degeneration occurs in the early stages of disease progression. Pathological studies of $SOD1^{G93A}$ mutant mice at multiple time points during the disease course showed that denervation of NMJs is significant far before the appearance of first pathological changes in the motor neurons.[3,4] Selective loss of fast fatigable neuromuscular synapses and resistance of slow-type synapses which retained high sprouting competence were also reported in mouse models of ALS.[5,6] The neurite outgrowth inhibitor Nogo-A, which is ectopically expressed in skeletal muscle of patients with ALS at levels that correlate with the severity of the clinical symptoms,[7] may play a role in this early loss of muscle innervation. In $SOD1^{G86R}$-mutant mice, Nogo-A is overexpressed in muscle[8] and its genetic ablation prolongs survival and reduces muscle denervation.[9] Furthermore, it has been shown that overexpression of Nogo-A in wild-type mouse muscle affects the NMJ with fragmentation of the postsynaptic compartment and loss of nerve–muscle contact.[9]

In patients with ALS, various studies using surface recording of compound motor action potentials (CMAPs) after repetitive nerve stimulation (RNS) at slow stimulus rate have suggested impairment of neuromuscular transmission.[10–14] However, the underlying morphological changes of the NMJs remain largely unknown. Using confocal and electron microscopy, we performed a comprehensive study of the structure of the NMJ in five early-stage ALS patients and four long-term survivors. We correlated the morphological results with electrophysiological and clinical data, and with the level of Nogo-A muscle content determined by western blot analysis. We showed that major structural alterations of the NMJs were present in all ALS patients and that NMJ loss of innervation correlated with Nogo-A muscle expression.

Patients and Methods

Patients and controls

Nine patients were enrolled in a study performed between March 2009 and July 2013. The study was approved by the local ethics committee and all patients provided written informed consent according to the institutional guidelines. All patients met the El Escorial World Federation of Neurology criteria for the diagnosis of definite, probable, or possible ALS.[15] With the patients' written informed consent, genetic screening was performed for mutations in the *SOD1*, *TARDBP*, and *FUS* genes, and for the GGGGCC hexanucleotide-repeat expansion in the *C9ORF72* gene. All patients were prospectively followed up every 3 months after muscle biopsy. Functional impairment was assessed using the revised ALS Functional Rating Scale (ALSFRS-R) which rates the performance of activities of daily living, with scores from 0 (total disability) to 48 (no disability).[16] The rate of disease progression from symptom onset was calculated for each patient as follows:

(48 − ALSFRS-R score at "last follow-up")/time from *symptom onset to last follow-up*

Surface-recorded neurotransmission studies

Surface-recorded studies of neuromuscular transmission were performed at the time of inclusion. The RNS test at slow stimulus rate (10 stimuli at 3 Hz) was performed at room temperature, bilaterally on the spinal accessory nerve (recording electrode over the upper trapezius muscle), the ulnar nerve (recording electrode over the hypothenar muscle), the radial nerve (recording electrode over the anconeus muscle), the deep peroneal nerve (recording electrode over the tibialis anterior muscle), and the cranial nerve V. For the cranial nerve V, the recording electrode was placed over the submandibular region (recording of the mylohyoid muscle which is innervated by a branch of the mandibular nerve) and the stimulation was performed below the angle of the mandible. For each train of repetitive stimuli, the amplitudes of the first and fifth CMAPs were compared, and the resulting decrement of the latter (if present) was expressed as a percentage. In clinical practice, a decrement greater than 10%, with a smooth U-shape, is considered to indicate neurotransmission impairment.[17] Short exercise tests were performed according to the technique described by Four-

nier and colleagues.[18] CMAPs were recorded on the hypothenar muscle after stimulation of the ulnar nerve at the wrist and on the plantar flexor muscles after stimulation of the posterior tibial nerve at the ankle. CMAPs were recorded at rest, and immediately after a maximal voluntary contraction of the muscle in isometric conditions during 30 sec. The procedure was repeated three times for each nerve. A postexercise increment greater than 20% was considered abnormal, suggesting presynaptic dysfunction.

Motor-point muscle biopsy procedure

Muscle samples were removed from the deltoid muscle by open biopsy under local anesthesia for six patients. The region containing NMJs was determined by the small twitch provoked by the tip of the scalpel on the surface of the muscle fascicles. For three patients, muscle specimens were taken from the anconeus muscle, under regional anesthesia, using the technique described by Maselli and colleagues.[19,20]

Confocal imaging study of NMJs

The presence of NMJs was confirmed on a longitudinal strip of the specimen using the classic Koelle method revealing cholinesterase activity.[21] After fixation with 4% paraformaldehyde, whole mounts of muscle specimens were stained for acetylcholine receptors (AChRs) with tetramethylrhodamine-conjugated α-bungarotoxin (1/500, Molecular Probes, Life Technologies, Saint Aubin, France). For staining of axons, the following primary antibodies were used: 168 kDa neurofilament antibody (1/250, 2H3, Developmental Studies Hybridoma Bank, Iowa City, IA), 200 kDa neurofilament antibody (1/250, Chemicon International Inc., Billerica, MA), and 68 kDa neurofilament antibody (1/100, Abcam, Cambridge, MA). Terminal Schwann cells (TSCs) were revealed by anti-S100 polyclonal antibody (1/50, Polyclonal Rabbit S100, Dako, Les Ulis, France). The specimens were observed by confocal microscopy (Carl Zeiss LSM510, Oberkochen, Germany).

Electron microscopy

Muscle samples were fixed in a mixture of paraformaldehyde 2% and glutaraldehyde 2.5% in 0.12 mol/L phosphate buffer (pH 7.4). Samples were postfixed with osmium tetroxide (2%) in sodium cacodylate buffer, dehydrated and embedded in epoxy resin. Ultrathin sections (80 nm) were contrasted with uranyl acetate followed by Reynolds lead citrate and viewed in a Philips CM120 transmission electron microscope (Philips Electronics Ltd., Amsterdam, the Netherlands). Digital images were taken with a Morada CCD camera (Soft Imaging Systems, Muenster, Germany).

Western blot determination of Nogo-A muscle content

For western blot determination of Nogo-A muscle content, total protein extracts were prepared as described previously.[8] Briefly, muscle biopsy specimens were manually homogenized in phosphate-buffered saline containing 1% Nonidet P-40, 0.5% sodium deoxycholate, 0.1% sodium dodecyl sulfate, 1% protease inhibitor cocktail, and 1% phosphatase inhibitor cocktail. Homogenates were boiled for 5 min and sonicated for 20 sec. After centrifugation at 15,000*g* for 20 min at 4°C, equal amounts of protein, according to the bicinchoninic acid assay, were separated at a constant voltage of 125 V with 4–20% Mini-PROTEAN® TGX™ Precast Gel (Bio-Rad, Marnes-la-Coquette, France) using manufacturer's instructions. Separated proteins were electrotransferred to nitrocellulose membranes using the Trans-Blot® Turbo™ Transfer Pack (Bio-Rad). Reversible staining with 0.1% Ponceau S in 5% acetic acid was performed as loading control and used for quantification purposes.[22] Rabbit polyclonal anti-Nogo-A antibody (AR2) was directed against sequence AKIQAKIPGLKRKAE, as described previously.[7] Mouse brain protein extract was systematically included to ensure Nogo-A band identification. Immunostaining was performed with AR2 diluted 1/2000 and horseradish peroxidase–conjugated goat anti-rabbit IgG (Abliance, Compiègne, France) diluted 1/5000. Blots were developed by enhanced chemiluminescence detection using Pierce SuperSignal West Pico (Thermo Fisher Scientific, Courtaboeuf, France), and visualized with ChemiDoc™ XRS+ imaging system (Bio-Rad). Nogo-A protein expression was quantified and normalized to Ponceau staining using Image Lab™ v5.1 software (Bio-Rad).

Statistical analysis

Statistical analysis was conducted with XLSTATS 2012 software (Addinsoft, Paris, France) and SAS software version 8.2 (SAS Institute, Cary, NC). We used the Mann–Whitney *U* test to compare continuous data. Correlations between CMAP variation during RNS and CMAP amplitude at rest were analyzed with a linear mixed model for correlated data. We used a linear mixed model for correlated data and a generalized linear mixed model for correlated data to compare the morphological modifications of the NMJs between ALS long-term survivors and rapidly progressive ALS patients. Correlations between Nogo-A muscle expression level, morphological characteristics, and electrophysiological and clinical data were analyzed using

Table 1. Demographic and clinical characteristics of ALS patients.

Patient no./sex	Site of disease onset	Age (years)	Disease duration at the time of muscle biopsy (months)	ALSFRS-R score at the time of muscle biopsy (months)	Follow-up duration (months)	Disease progression rate[1] (units/month)
1/F	Spinal	63	10	35	39	0.7
2/M	Spinal	50	12	37	1	1.4
3/F	Bulbar	60	9	42	16	1.5
4/F	Spinal	48	9	30	34	2.7
5/M	Bulbar	56	14	39	13	0.9
6/M	Spinal	53	193	32	27	0.1
7/F	Spinal	36	85	32	28	0.2
8/M	Spinal	52	101	37	28	0.1
9/F[2]	Spinal	55	100	41	26	0.1
All patients[3]		53	14	36	24	0.9

Patients 6–9 met the criteria for long-term ALS survivors.[23] Mean disease progression rate was significantly different between the rapidly progressive ALS group and the long-term ALS survivors group (1.4 and 0.1 units/month, respectively, $P = 0.016$). ALSFRS-R, revised ALS Functional Rating Scale.

[1]Disease progression rate from symptom onset = (48 – ALSFRS-R score at "last follow-up") / time from symptom onset to last follow-up.

[2]Mutation on the *SOD1* gene (c.418A>G, amino acid numbering according to the ALS online database: N139D).

[3]Values are means, except for disease duration (median disease duration at the time of the biopsy).

the nonparametric Spearman rank correlation test. All statistics were two-tailed and the level of significance was set at $P = 0.05$.

Results

Characteristics of patients with ALS

Nine patients were included in this study (Table 1). All patients were treated with riluzole. Median disease duration at the time of the biopsy was 10 months for five patients with early-stage ALS. Median disease duration was 100 months for four patients who had more than 5 years of disease progression without requiring respiratory support or gastrostomy feeding and met the definition for long-term ALS survivors.[23]

Major morphological alterations of the NMJs are present in all patients with ALS

Postsynaptic apparatus morphology

The postsynaptic apparatus was abnormal in all ALS patients for almost all detectable NMJs ($n = 430$) observed under confocal microscopy (Fig. 1). Denervation-induced modifications included enlargement, fragmentation, and flattening of the postsynaptic apparatus. Most of the NMJs showed a fragmented postsynaptic compartment, with at least two distinct postsynaptic elements that could be individualized (Fig. 1B–E, Table 2). In some NMJs, staining of AChRs was barely detectable, usually in the case of complete denervation. In some cases, the outer edge of the postsynaptic primary gutter presented spike-like areas of AChR labeling (Fig. 1D). On electron micrographs, the primary synaptic clefts were usually flattened with relatively well-preserved secondary synaptic clefts (Fig. 2). The presence of AChRs was identified as a dark electron-opaque border on the crests of the subneural folds. In some NMJs, this dark electron-opaque border extended to the immediately adjacent, unfolded, portion of the postsynaptic membrane, paralleling the spiculated aspect observed under confocal microscope after AChR labeling (Fig. 2D).

Quantitative and qualitative analysis of innervation

Of the 228 NMJs analyzed under confocal microscopy (Fig. 3), 45 (19.7%) were completely denervated (i.e., fragmented synaptic gutters and absence of nerve terminal profile). Among the remaining 183 innervated NMJs, 79 (43.2%) were "remodeled" NMJs in which the axon terminal partially innervated a flattened, fragmented postsynaptic apparatus. One hundred and four NMJs (56.8%) were reinnervated (i.e., NMJs associating a flattened and fragmented postsynaptic apparatus and one of the following patterns of reinnervation: nodal, preterminal, or ultraterminal sprouting, reinnervation with a single axon terminal innervating several cups with or without branching).

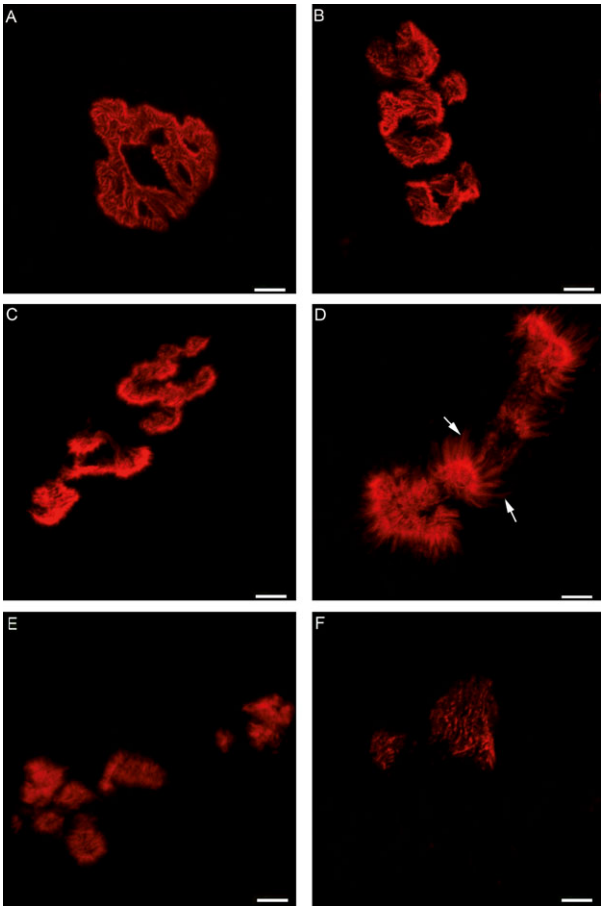

Figure 1. Morphology of the postsynaptic apparatus observed by confocal microscopy (α-Bungarotoxin staining of AChRs, in red). (A) Normal, "pretzel-shaped," postsynaptic apparatus. (B–E) Denervation-induced modifications of the postsynaptic apparatus. Fragmentation and enlargement of the postsynaptic apparatus with flattening of the primary synaptic gutter. The outer edge of the postsynaptic primary gutter sometimes showed spike-like areas (D, arrows). (F) Barely visible postsynaptic apparatus, usually seen in the absence of contact with a nerve terminal profile, that is, completely denervated NMJ. Scale bars, 5 μm. AChR, acetylcholine receptor; NMJ, neuromuscular junction.

We then studied the morphology of all innervated NMJs in which innervation characteristics could be determined ($n = 107$). Normal NMJs, with a normal postsynaptic apparatus facing a normal terminal arborization, were not seen. For each innervated NMJ, we determined the following parameters: number of axons per NMJ, number of first-order branches of the terminal arborization, and number of sprouts (regrouping nodal, preterminal and ultraterminal sprouts) per axon (Table 2). Each NMJ was usually singly innervated, but some NMJs, particularly in the long-term ALS survivors, were polyinnervated. The number of axons per NMJ correlated positively with disease duration ($P = 0.025$, $r = 0.749$) and negatively with disease progression rate ($P = 0.031$, $r = -0.730$). Each terminal axon gave rise to a mean of 1.02 sprouts. The mean number of first-order branches of the terminal arborization was 1.10 and correlated negatively with the proportion of reinnervated NMJs ($P = 0.050$, $r = -0.681$). Innervation characteristics were similar in both ALS groups (Table 2).

Terminal Schwann cell alterations

Using confocal microscopy, we analyzed the TSC morphology of 51 NMJs (Table 2, Fig. 4). Most of the TSCs were abnormal with extensive cytoplasmic processes. On average, TSCs extended 2.22 processes and contacted 1.90 distinct postsynaptic elements. TSC alterations were similar in both ALS groups. On electron micrographs, TSCs normally "capped" the nerve terminal in some NMJs (Fig. 2B–D), but in others a marked interposition of the TSC between the axon terminal and the postsynaptic membrane could be observed, which was sometimes so pronounced that only a small part of the synaptic surface was accessible for neuromuscular transmission (Fig. 5). Multiple layers of TSC basal lamina were often visible near the primary synaptic cleft (Fig. 2B).

Assessment of neuromuscular transmission

A decrement of CMAP amplitude was observed in 44/86 nerves after RNS (Table S1). The size of the decrement correlated negatively with the CMAP amplitude at rest ($P = 0.005$, $\beta = 0.73$). We did not observe any correlation between the morphological features of the NMJs and the magnitude of the CMAP decrement measured on the same muscle (for anconeus biopsies) or a muscle of the same region (trapezius, for deltoid biopsies). Three patients, among whom two were long-term ALS survivors, showed a CMAP decrement greater than 10% in at least one muscle/nerve combination. In these patients, the size of the decrement ranged from 16% to 26% (mean 20%). During short exercise tests, immediate postexercise abnormal facilitation (reflecting presynaptic alterations of the neuromuscular transmission) was not detected.

Nogo-A muscle upregulation is associated with a higher proportion of denervated NMJs and a faster functional decline

Muscle Nogo-A relative protein content could be quantified by western blot analysis in 7/9 patients (Fig. 6). In these patients, Nogo-A muscle content correlated negatively with the disease duration at the time of the biopsy ($P = 0.012$, $r = -0.893$). Nogo-A muscle expression level

Table 2. Morphological characteristics of NMJs of ALS patients.

Patient no.	1 (n = 34)	2 (n = 68)	3 (n = 61)	4 (n = 41)	5 (n = 41)	Early ALS patients	6 (n = 58)	7 (n = 70)	8 (n = 22)	9 (n = 35)	Long-term survivors
Fragmentation (% of NMJs analyzed)[1]	69.23	95.65	95.83	100	90	90.14	91.43	73.53	100	90.48	88.86
Mean number of axons per NMJ	1	1	1	1	1.07	1.01	1.09	1.04	1.13	1	1.06
Mean number of first-order branches per axon	0.63	1	1.09	1.63	0.93	1.05	1.79	0.91	0.89	0.36	1.14
Mean number of sprouts per axon	0.25	0.5	1.36	1.25	1.4	1.11	1.38	0.42	1.56	0.73	0.96
Mean number of postsynaptic elements per TSC	2.22	1.86	1.57	1.63	1	2.18	2.58	2	3	1	1.75
Mean number of processes per TSC	2	1.96	2.67	3	ND	2.24	2.38	2.17	2	2	2.21

Values are presented as means for both groups. Differences between groups were not statistically significant. Patients 1–5: early ALS patients; patients 6–9: long-term ALS survivors. n, number of NMJs analyzed for each patient. NMJ, neuromuscular junction; ALS, amyotrophic lateral sclerosis; TSC, terminal Schwann cell; ND, not determined.

[1]Pathological fragmentation: proportion of NMJs with at least two individualized postsynaptic elements.

correlated positively with the disease progression rate, with a higher Nogo-A muscle content being associated with a faster functional decline ($P = 0.012$, $r = 0.893$). The proportion of denervated NMJs determined on muscle specimens correlated with Nogo-A protein level, a higher Nogo-A muscle content being associated with a greater endplate denervation ($P = 0.03$, $r = 0.821$). No statistically significant correlation was observed between Nogo-A muscle expression and the other morphological parameters. However, there was trend for a higher Nogo-A muscle expression level being associated with a greater fragmentation of the postsynaptic apparatus (i.e., a higher proportion of NMJs showing a fragmented postsynaptic compartment, $P = 0.088$, $r = 0.703$) and a lower proportion of reinnervated NMJs ($P = 0.066$, $r = -0.739$).

Discussion

In this work, we showed that major alterations of NMJ morphology were present in all patients with ALS, affecting the three cell components of the NMJ: the postsynaptic apparatus, the axon terminal, and the TSC. These alterations were seen both in long-term survivors and in early-stage ALS patients, confirming in humans that NMJ degeneration occurs early in the disease process as suggested in animal models.[3,4]

In agreement with previous reports,[24–26] we observed denervation-induced modifications on electron micrographs, with fragmentation and flattening of the postsynaptic apparatus, and reduced innervation with fairly well-preserved secondary synaptic clefts. These alterations are not specific to ALS and may be encountered in other diseases with a denervation process. Other morphological modifications have not been reported, to date, in ALS. After staining of AChRs, some NMJs presented spikes running out from the edges of the postsynaptic primary gutter. Consistent with this observation, ultrastructural examination of some NMJs showed that the presence of AChRs seemed to extend to the immediately adjacent, but unfolded, portion of the postsynaptic membrane. This morphological appearance of NMJs has been observed in mice deficient in α-dystrobrevin, a protein involved in the anchoring of AChRs, and thus in the maturation and stabilization of the postsynaptic membrane.[27] Such spikes were also reported in mice with deficient neuregulin/ErbB signaling, which contributes to the stabilization of the postsynaptic apparatus via phosphorylation of α-dystrobrevin.[28] In ALS patients, these spikes may thus be seen, during the denervation/reinnervation process, in "incompletely" matured NMJs.

Multiple layers of TSC basal lamina were often visible near the primary synaptic clefts. This accumulation of

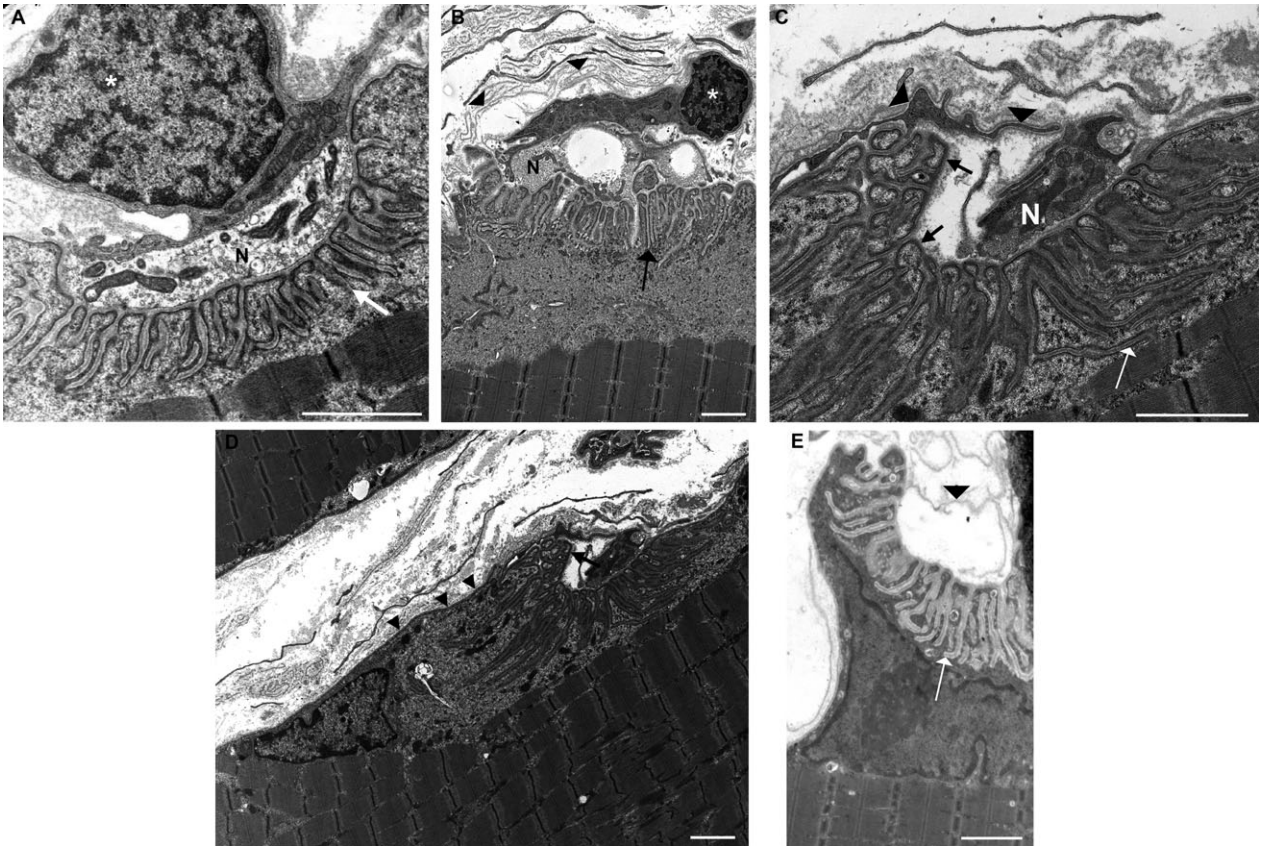

Figure 2. Ultrastructural findings at the neuromuscular junction (NMJ). (A) Control and (B–E) patients with amyotrophic lateral sclerosis (ALS). (A) Normal NMJ from a control subject. The primary synaptic gutter is occupied by a nerve terminal (N) containing numerous synaptic vesicles and mitochondria. Note the postsynaptic membrane folding with well-formed secondary synaptic clefts (arrow). The terminal Schwann cell (TSC) caps the nerve terminal, without extending into the synaptic cleft (the asterisk is placed over the TSC nucleus). (B) A flattened primary synaptic gutter with well-preserved subneural folds (arrow) faces a remodeled motor nerve terminal. The vacuoles within the nerve ending (N) are probably artifacts. The TSC caps the nerve terminal (star: TSC nucleus). Multiple layers of TSC basal lamina can be seen near the primary synaptic cleft (arrowheads). (C–E) Denervated NMJs. (C) Partially denervated NMJ. A small nerve terminal profile (N) partially occupies the primary synaptic gutter. Note the well-preserved secondary synaptic clefts (white arrow) and the TSC capping the nerve terminal (arrowheads). The presence of acetylcholine receptors (AChRs) on the crests of the subneural folds is identified as an electron-opaque border (black arrows). (D) Same NMJ as in B, lower magnification. On the crests of the subneural folds, where AChRs are present, the muscle postsynaptic membrane shows an electron-opaque border (arrow). Here, this dark border extends to the immediately adjacent, unfolded, postsynaptic membrane (arrowheads). (E) Fully denervated NMJ. Unoccupied synaptic gutter with absence of nerve terminal and well-preserved subneural folds (arrow). Residual TSC basal lamina can be seen in the remaining primary synaptic cleft (arrowhead). Scale bars, 2 μm.

TSC laminae is thought to be a consequence of repeated episodes of expansion/contraction of TSC during the NMJ regeneration process,[29] and could be associated with recurrent episodes of denervation and reinnervation encountered in ALS.[30] Following experimental denervation, TSCs of the denervated endplates grow cytoplasmic processes to form bridges with neighboring innervated NMJs, bridges that will guide reinnervation. Reinnervation results in a withdrawal of all the processes except those used by the regenerating axon to reinnervate a postsynaptic apparatus.[31,32] Consistently, in our study, TSCs elaborated extensive cytoplasmic processes contacting distinct postsynaptic elements.

Under confocal microscope, more than half of innervated NMJs showed a characteristic reinnervation pattern, confirming the importance of compensatory reinnervation in ALS.[33–35] As a result of the collateral reinnervation process, endplate polyinnervation was observed in some NMJs and correlated with a higher disease duration and a lower progression rate. In addition, the terminal axonal arborization was usually sparsely branched, possibly related to "immaturity" of reinnervated NMJs. Consis-

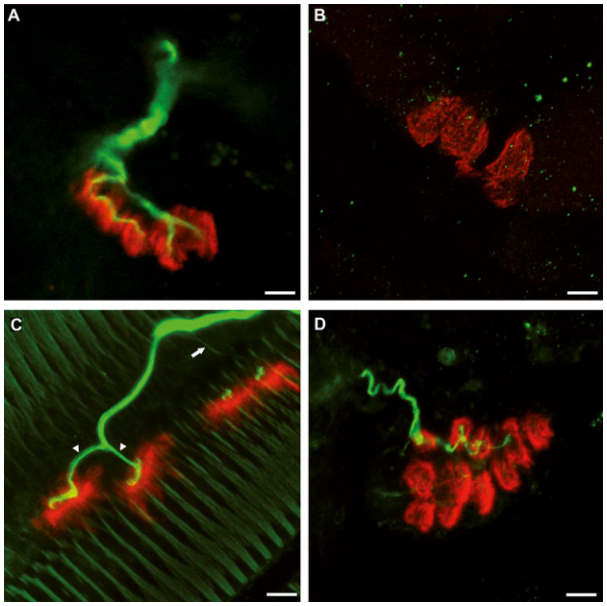

Figure 3. Neuromuscular junctions (NMJs) observed by confocal microscopy. Staining of acetylcholine receptors (AChRs) with α-bungarotoxin, in red, and of axon terminals with neurofilament antibody, in green. (A) Normal NMJ from one control (profile view). The motor axon divides into two first-order branches. (B) Fully denervated NMJ with no axon. Note the low AChR staining of the postsynaptic compartment. (C) Reinnervated NMJ. A fragmented postsynaptic apparatus is innervated by a motor axon which divides into two first-order branches (arrowheads). Note the fine nodal sprout reinnervating two postsynaptic elements (arrow). (D) Remodeled, partially innervated NMJ. The axon terminal partially innervates a slightly flattened postsynaptic apparatus. Scale bars, 5 μm.

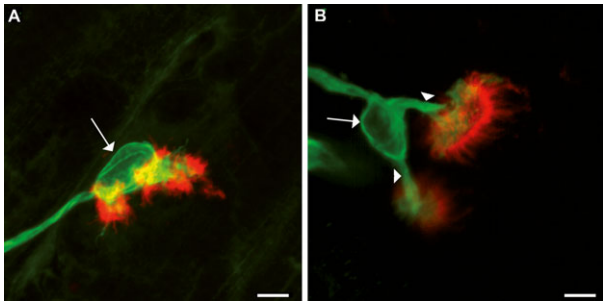

Figure 4. Neuromuscular junctions (NMJs) observed by confocal microscopy after staining of acetylcholine receptors (AChRs) with α-bungarotoxin, in red, and of terminal Schwann cells (TSCs) with anti-S100 antibody, in green. (A) A TSC (arrow) caps a postsynaptic apparatus made of two adjacent synaptic cups. There are no Schwann cell cytoplasmic processes. (B) A TSC (arrow) elaborates two cytoplasmic processes (arrowheads), each process contacting one isolated postsynaptic element. Scale bars, 5 μm.

tently, the mean number of first-order branches per axon at a given NMJ correlated inversely with the proportion of reinnervated NMJs.

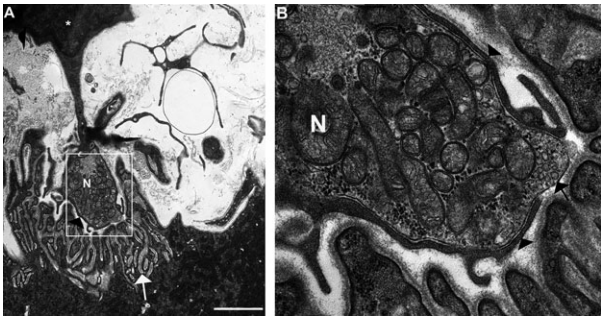

Figure 5. Electron microscopy view showing an interposition of the terminal Schwann cell (TSC) between the axon terminal and the postsynaptic muscle membrane. (A, B) The membrane of the TSC (star) invades the synaptic cleft (arrowhead) and encases the nerve terminal (N). Secondary synaptic clefts are maintained (white arrow). Note in (B) that the area of the muscle postsynaptic membrane facing the residual part of the nerve terminal (black arrow), available for neurotransmission, is very narrow. Scale bar, 2 μm.

To identify clinically relevant impairment of neuromuscular transmission, we performed RNS tests at slow stimulus rate, a technique commonly used for the assessment of neuromuscular transmission in the case of muscle weakness.[17] We found a CMAP decrement greater than 10% after RNS, indicating NMJ functional alteration in clinical practice,[17] in a third of our patients. We did not detect immediate postexercise facilitation, unlike what is classically observed in disorders with presynaptic NMJ dysfunction.[36] Decremental motor responses to RNS in ALS has usually been attributed to a neuromuscular transmission dysfunction caused by "immaturity" of newly reinnervated structures.[13,37] Our results do not favor this hypothesis as the magnitude of the CMAP decrement did not correlate with the proportion of reinnervated NMJs in the same muscle or a muscle of the same region. Alternatively, synaptic transmission failure at NMJs undergoing degeneration (which may be either native or formerly reinnervated NMJs) may play a part in decremental responses recorded in patients with ALS. Abnormal interposition of the TSC in the synaptic cleft may also contribute to NMJ functional alteration and pathological decrement in ALS patients, by reducing the synaptic surface available for neurotransmission. This aspect is reminiscent of ultrastructural abnormalities observed in congenital myasthenic syndromes caused by human mutations on three major proteins of the basal lamina, that is, laminin β2, ColQ, and agrin. In these syndromes, invasion of the primary synaptic cleft by TSC processes is observed, with nerve terminals partially encased by Schwann cell projections.[38] Defects in synaptic basal lamina may thus be involved in ALS, particularly in laminin β2 that has been shown to actively inhibit TSC entry into the synaptic cleft.[39]

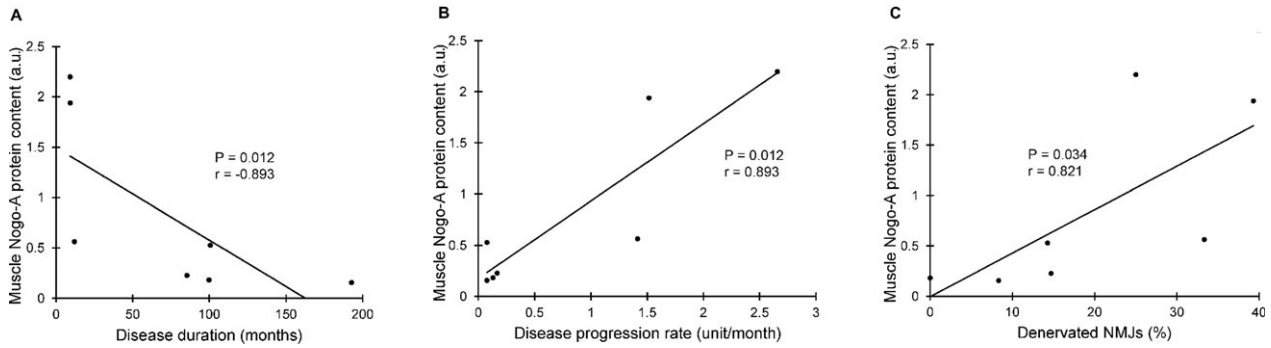

Figure 6. High-level expression of Nogo-A in muscle is associated with a faster functional decline and a higher proportion of denervated neuromuscular junctions (NMJs). Nogo-A muscle protein level, determined by the optical density of the Nogo-A signal bands normalized to the Red Ponceau staining (a.u.: arbitrary units), correlated negatively with the disease duration, and positively with the disease progression rate and the proportion of denervated NMJs. (A) Negative correlation between muscle Nogo-A protein content and disease duration at the time of the biopsy (Spearman rank correlation $r = -0.893$). (B) Positive correlation between muscle Nogo-A protein level and the disease progression rate from symptom onset (Spearman rank correlation $r = 0.893$). (C) Positive correlation between muscle Nogo-A protein level and the proportion of denervated NMJs (Spearman rank correlation $r = 0.821$).

Finally, we showed that high-level expression of Nogo-A in muscle significantly correlated with a greater extent of NMJ denervation. A high Nogo-A protein content in muscle was also associated with a higher proportion of NMJs showing a fragmented postsynaptic compartment, even if it did not reach statistical significance. We did not find any correlation between Nogo-A muscle expression level and the other morphological parameters investigated (i.e., innervation or TSC characteristics). These findings are consistent with the results of a previous study in which Nogo-A overexpression in wild-type muscle fibers led to endplate denervation and fragmentation of the postsynaptic compartment, suggesting that the high expression of Nogo-A in ALS muscle could affect the integrity of the NMJ, leading to its "destabilization" and to retraction of the nerve terminal.[9] In our study, in addition to being associated with NMJ denervation, Nogo-A muscle overexpression significantly correlated with a negative functional outcome. Our results are thus in agreement with a recent study showing that treatment with anti-Nogo-A antibody improved endplate innervation in hindlimb muscles and delayed disease progression in a mouse model of ALS.[40]

Altogether, our results show that major morphological defects are present in NMJs of patients with ALS even at the early stages. Muscle Nogo-A overexpression may contribute to NMJ denervation, and further work is now required to elucidate the molecular mechanisms mediating pre- and postsynaptic pathology. These NMJ alterations may significantly contribute to functional motor impairment and targeting this aspect of neurodegeneration could represent a potential therapeutic approach in ALS. A phase II study of the efficacy and safety of a humanized monoclonal antibody against Nogo-A in ALS patients (NCT01753076) is currently underway.

Acknowledgments

The authors thank all the patients who participated in this study and their relatives. The authors also thank Sylvie Dirrig-Grosch for efficient technical assistance. The study was conducted at the Neurosciences Clinical Research Centre (INSERM, CIC-1422), Pitié-Salpêtrière Hospital, Paris, France. This work was supported by the Association Française pour la Recherche sur la SLA (ARSla, AO 2007 – NETALS; G. B., D. H.), the Association Française contre les Myopathies (AFM, AO 2008 – no. 13501; G. B.), the Agence Nationale de la Recherche (ANR, program "Investissements d'avenir" ANR-10-IA-IHU-06; D. H., B. F.), the European Community's Health Seventh Framework Programme under Grant agreement no. 259867 (J.-P. L.), and a "Contrat d'interface" Inserm/APHP to G. B. Jose Luis Gonzalez de Aguilar is the recipient of a "Chaire d'Excellence INSERM/Université de Strasbourg." The funders' of the study had no role in study design, data collection and analysis, decision to publish, or preparation of the manuscript.

Author Contribution

G. B. (corresponding author) designed the study, was principally responsible for the clinical operations, performed experiments, analyzed data, and wrote the manuscript. S. B., J. L. G. D. A., G. H., G. Brochier, and N. M. performed experiments and analyzed data. M.-L. T. was principally responsible for the statistical analysis of

the study and participated in the writing of the manuscript. A. B., F. K., E. S. and C. H.-R. participated in the project design and performed muscle biopsies. F. S. and P.-F. P. participated in the clinical operations and writing of the manuscript. L. L., S. N., B. F., M. F., J.-P. L., J. K., E. F., and V. M. participated in the project design and discussed the results and implications. D. H. supervised the project design, data analysis, and manuscript preparation. All authors approved the final manuscript before submission.

Conflict of Interest

None declared.

References

1. Charcot JM, Joffroy A. Deux cas d'atrophie musculaire progressive avec lésions de la substance grise et des faisceaux antéro-latéraux de la moelle épinière. Arch Physiol 2015;2:362–372.
2. Beghi E, Mennini T, Bendotti C, et al. The heterogeneity of amyotrophic lateral sclerosis: a possible explanation of treatment failure. Curr Med Chem 2007;14:3185–3200.
3. Fischer LR, Culver DG, Tennant P, et al. Amyotrophic lateral sclerosis is a distal axonopathy: evidence in mice and man. Exp Neurol 2004;185:232–240.
4. Vinsant S, Mansfield C, Jimenez-Moreno R, et al. Characterization of early pathogenesis in the SOD1(G93A) mouse model of ALS: Part II, results and discussion. Brain Behav 2013;3:431–457.
5. Frey D, Schneider C, Xu L, et al. Early and selective loss of neuromuscular synapse subtypes with low sprouting competence in motoneuron diseases. J Neurosci 2000;20:2534–2542.
6. Pun S, Santos AF, Saxena S, et al. Selective vulnerability and pruning of phasic motoneuron axons in motoneuron disease alleviated by CNTF. Nat Neurosci 2006;9:408–419.
7. Jokic N, Gonzalez de Aguilar JL, Pradat PF, et al. Nogo expression in muscle correlates with amyotrophic lateral sclerosis severity. Ann Neurol 2005;57:553–556.
8. Dupuis L, Gonzalez de Aguilar JL, di Scala F, et al. Nogo provides a molecular marker for diagnosis of amyotrophic lateral sclerosis. Neurobiol Dis 2002;10:358–365.
9. Jokic N, Gonzalez de Aguilar JL, Dimou L, et al. The neurite outgrowth inhibitor Nogo-A promotes denervation in an amyotrophic lateral sclerosis model. EMBO Rep 2006;7:1162–1167.
10. Denys EH, Norris FH Jr. Amyotrophic lateral sclerosis. Impairment of neuromuscular transmission. Arch Neurol 1979;36:202–205.
11. Henderson R, Baumann F, Hutchinson N, McCombe P. CMAP decrement in ALS. Muscle Nerve 2009;39:555–556.
12. Killian JM, Wilfong AA, Burnett L, et al. Decremental motor responses to repetitive nerve stimulation in ALS. Muscle Nerve 1994;17:747–754.
13. Wang FC, De Pasqua V, Gerard P, Delwaide PJ. Prognostic value of decremental responses to repetitive nerve stimulation in ALS patients. Neurology 2001;57:897–899.
14. Yamashita S, Sakaguchi H, Mori A, et al. Significant CMAP decrement by repetitive nerve stimulation is more frequent in median than ulnar nerves of patients with amyotrophic lateral sclerosis. Muscle Nerve 2012;45:426–428.
15. Brooks BR, Miller RG, Swash M, Munsat TL. El Escorial revisited: revised criteria for the diagnosis of amyotrophic lateral sclerosis. Amyotroph Lateral Scler Other Motor Neuron Disord 2000;1:293–299.
16. Cedarbaum JM, Stambler N, Malta E, et al. The ALSFRS-R: a revised ALS functional rating scale that incorporates assessments of respiratory function. BDNF ALS Study Group (Phase III). J Neurol Sci 1999;169:13–21.
17. AAEM. Practice parameter for repetitive nerve stimulation and single fiber EMG evaluation of adults with suspected myasthenia gravis or Lambert-Eaton myasthenic syndrome: summary statement. Muscle Nerve 2001;24:1236–1238.
18. Fournier E, Arzel M, Sternberg D, et al. Electromyography guides toward subgroups of mutations in muscle channelopathies. Ann Neurol 2004;56:650–661.
19. Maselli RA, Mass DP, Distad BJ, Richman DP. Anconeus muscle: a human muscle preparation suitable for in-vitro microelectrode studies. Muscle Nerve 1991;14:1189–1192.
20. Maselli RA, Wollman RL, Leung C, et al. Neuromuscular transmission in amyotrophic lateral sclerosis. Muscle Nerve 1993;16:1193–1203.
21. Koelle GB, Friedenwald JA. A histochemical method for localizing cholinesterase activity. Proc Soc Exp Biol Med 1949;70:617–622.
22. Romero-Calvo I, Ocon B, Martinez-Moya P, et al. Reversible Ponceau staining as a loading control alternative to actin in Western blots. Anal Biochem 2010;401:318–320.
23. Mateen FJ, Carone M, Sorenson EJ. Patients who survive 5 years or more with ALS in Olmsted County, 1925-2004. J Neurol Neurosurg Psychiatry 2010;81:1144–1146.
24. Bjornskov EK, Dekker NP, Norris FH Jr, Stuart ME. End-plate morphology in amyotrophic lateral sclerosis. Arch Neurol 1975;32:711–712.
25. Tsujihata M, Hazama R, Yoshimura T, et al. The motor end-plate fine structure and ultrastructural localization of acetylcholine receptors in amyotrophic lateral sclerosis. Muscle Nerve 1984;7:243–249.
26. Yoshihara T, Ishii T, Iwata M, Nomoto M. Ultrastructural and histochemical study of the motor end plates of the

intrinsic laryngeal muscles in amyotrophic lateral sclerosis. Ultrastruct Pathol 1998;22:121–126.
27. Grady RM, Akaaboune M, Cohen AL, et al. Tyrosine-phosphorylated and nonphosphorylated isoforms of alpha-dystrobrevin: roles in skeletal muscle and its neuromuscular and myotendinous junctions. J Cell Biol 2003;160:741–752.
28. Schmidt N, Akaaboune M, Gajendran N, et al. Neuregulin/ErbB regulate neuromuscular junction development by phosphorylation of alpha-dystrobrevin. J Cell Biol 2011;195:1171–1184.
29. Couteaux R, Mira JC, d'Albis A. Regeneration of muscles after cardiotoxin injury. I. Cytological aspects. Biol Cell 1988;62:171–182.
30. Meriggioli MN, Howard JFJ, Harper CMJ. Pathophysiology of neuromuscular junction disorders. In: Dekker M, ed. Neuromuscular junction disorders: diagnosis and treatment. New York: CRC Press, 2003: pp.37–57.
31. Son YJ, Thompson WJ. Nerve sprouting in muscle is induced and guided by processes extended by Schwann cells. Neuron 1995;14:133–141.
32. O'Malley JP, Waran MT, Balice-Gordon RJ. In vivo observations of terminal Schwann cells at normal, denervated, and reinnervated mouse neuromuscular junctions. J Neurobiol 1999;38:270–286.
33. Coers C. Histological aspects of neuromuscular regeneration during various diseases of the peripheral motor neuron; collateral regeneration in humans. Acta Neurol Psychiatr Belg 1955;55:23–30.
34. Wohlfart G. Collateral regeneration from residual motor nerve fibers in amyotrophic lateral sclerosis. Neurology 1957;7:124–134.
35. Fardeau M. Simultaneous staining of the terminal motor innervation and the sub-neural apparatus (S. Manolov's technic). Importance for diagnosis in neuro-muscular pathology. Rev Neurol (Paris) 1964;111:501–506.
36. O'Neill JH, Murray NM, Newsom-Davis J. The Lambert-Eaton myasthenic syndrome. A review of 50 cases. Brain 1988;111(Pt 3):577–596.
37. Stalberg E. Electrophysiological studies of reinnervation in ALS. Adv Neurol 1982;36:47–59.
38. Maselli RA, Arredondo J, Ferns MJ, Wollmann RL. Synaptic basal lamina-associated congenital myasthenic syndromes. Ann N Y Acad Sci 2012;1275:36–48.
39. Patton BL, Chiu AY, Sanes JR. Synaptic laminin prevents glial entry into the synaptic cleft. Nature 1998;393:698–701.
40. Bros-Facer V, Krull D, Taylor A, et al. Treatment with an antibody directed against Nogo-A delays disease progression in the SOD1G93A mouse model of amyotrophic lateral sclerosis. Hum Mol Genet 2014;23:4187–4200.

Supporting Information

Additional Supporting Information may be found in the online version of this article:

Table S1. Surface-recording study of neuromuscular transmission: results of RNS tests at the time of inclusion.

